THE LHC MAGNETIC FIELD MODEL

N. Sammut, CERN, Geneva, Switzerland; University of Malta, Malta
L. Bottura, CERN, Geneva, Switzerland
J. Micallef, University of Malta, Malta

Abstract

The compensation of the field changes during the beam injection and acceleration in the LHC requires an accurate forecast and an active control of the magnetic field in the accelerator. The LHC Magnetic Field Model is the core of this magnetic prediction system. The model will provide the desired field components at a given time, magnet operating current, magnet ramp rate, magnet temperature and magnet powering history to the required precision. The model is based on the identification and physical decomposition of the effects that contribute to the total field in the magnet aperture of the LHC dipoles. Each effect is quantified using data obtained from series measurements, and modeled theoretically or empirically depending on the complexity of the physical phenomena involved. This paper presents the developments of the new finely tuned magnetic field model and evaluates its accuracy and predictive capabilities over a sector of the machine.

MATHEMATICAL FORMULATION

The field model is a decomposition of the field errors and their deviations from the reference design values based on a separation of the contributing effects. We indicate with $\mathbf{C}_n$ the complex harmonic of order n in the complex series expansion of the 2-D magnetic field in the magnet aperture [1]. The coefficients $\mathbf{C}_n$ have dimensions of [T @ R_{ref}]. The order of the main field is m = 1 for a dipole, and the index n stands for the higher order field harmonics, i.e. $n \geq m+1$.The main field is indicated as B_m (in T at the reference radius R_{ref} =17mm). For convenience, we use also normalized harmonic coefficients, indicated as $\mathbf{c}_n$ and defined as:

$$\mathbf{c}_n = b_n + ia_n = 10^4 \frac{\mathbf{C}_n}{B_m} \tag{1}$$

expressed in [units @ R_{ref}], and decomposed in their real part b_n (the normal harmonics) and imaginary part a_n (the skew harmonics). Finally, the main field transfer function (*TF*) is defined as the ratio of field generated and operating current:

$$TF = \frac{B_m}{I} \tag{2}$$

which is expressed in units of [T @R_{ref} / A]. The field model is the relation:

$$\mathbf{C}_n = \mathbf{C}_n\left(t, I, \frac{dI}{dt}, T, I(-t)\right) \tag{3}$$

where we express the fact that the harmonic $\mathbf{C}_n$ depends on time (t), magnet operating current (I), magnet ramp-rate (dI/dt), magnet temperature (T) and magnet powering history $I(-t)$. To give an explicit form of the field model, we decompose the field errors in the following components:

1) DC Components $\mathbf{c}_n^{DC}$ (steady state, reproducible from cycle to cycle, depend on current, but not on time)

a. *Residual Magnetization Contribution:* permanent magnetization of magnetic parts in the cold mass, mostly in the iron surrounding the coils, which are visible at low current, e.g. during warm measurements. This effect is modeled empirically using the equation:

$$\mathbf{c}_n^{residual} = \rho_n \left(\frac{I_{inj}}{I}\right)^{\zeta_n} \tag{4}$$

where the measurement injection current I_{inj} is introduced to normalize the equation and ρ_n and ζ_n are the fitting parameters.

b. *Geometric Contribution*: deviation between the conductor placement in the real coil winding and the ideal distribution of current (i.e. producing the exact, desired multipolar field). This contribution is present at all field levels and is proportional to the operating current. This effect is identified using:

$$\mathbf{c}_n^{geometric} = \gamma_n \tag{5}.$$

The geometric coefficient γ_n, in its definition above, also includes the linear contribution from the iron yoke (i.e. ignoring the saturation and permanent magnetization). This is the only component of the model that can be obtained through extrapolation from warm measurements.

c. *Displacement Contribution:* displacement of the cables in the coil cross-section. Cable movements can take place, for instance, during cool-down and powering at high field as a consequence of the changes in the force and stress distribution.

d. *Saturation Contribution*: changes of the magnetic permeability in the iron yoke surrounding the coils. This contribution is important at high fields and appears as a non-linearity of the field and field errors with respect to the operating current.

The saturation and the displacement contributions are empirically modeled together by:

$$\mathbf{c}_n^{sat} = \sum_{n=1}^{N} \sigma_n \left[\frac{1}{}\text{atan}\left(\upsilon_n\left(\frac{I-\xi_n}{I_{nom}}\right)\right)+\frac{1}{2}\right] \tag{6}$$

where N is typically 1 or 2 depending on the harmonic. The nominal current I_{nom} is used to normalize the equation and σ_n , υ_n and ξ_n are the fitting parameters.

e. *DC Magnetization Contribution*: persistent currents in the superconducting filaments. This contribution is important at low operating field (e.g. injection in the main dipoles), where the superconductor magnetization is highest. In the first approximation, the magnetization is proportional to the critical current density J_c and the filament diameter D [2] :

$$M \propto J_c D \tag{7}$$

The critical current density changes with field according to a law of the type [3]:

$$J_c \propto \frac{1}{B}\left(\frac{B}{B_c(T)}\right)^{\alpha_n}\left(1-\frac{B}{B_c(T)}\right)^{\beta_n}\left(1-\left(\frac{T}{T_{co}}\right)^{1.7}\right)^2 \tag{8}$$

where B is the background field, B_c is the critical field of the material, T is the temperature, T_{co} is the critical temperature and α_n and β_n are pinning exponents that are typically in the range of 0.5 and 1.5 for the NbTi alloy used in the LHC cables.

M is essentially stationary in time (dc) and is hysteretic since the persistent currents have exceedingly long time constants. Hence, the dc magnetization is visible as a hysteretic contribution to the field and field errors that depends on the strength of the magnetization as well as on the geometric distribution of the magnetization vectors in the winding cross section. Smaller magnetization amplitudes in the high-field regions and larger magnetization in the low-field regions are the result of the presence of large field gradients in the coil. In particular, this is important at injection where the magnitude and variation of M is the largest. The current is substituted for field yielding:

$$\mathbf{c}_n^{MDC} = \mu_n\left(\frac{I_{inj}}{I}\right)^{2-\alpha_n}\left(\frac{I_c - I}{I_c - I_{inj}}\right)^{\beta_n}\left(\frac{T_{co}^{1.7} - T^{1.7}}{T_{co}^{1.7} - T_m^{1.7}}\right)^2 \tag{9}$$

where the measurement injection current I_{inj} and the measured temperature T_m are introduced as reference points so that the product of the three terms in I is equal to the one at I_{inj}, and the term in T is equal to 1 at T_m. The value of μ_n can be interpreted as the value of the contribution of the dc magnetization to the total field measured at injection, and presently stored in the database. By writing Eq. (9) we assume that the complex convolution of the distribution of magnetization vectors can be condensed in the fitting exponents α_n and β_n.

2) AC Short Term Effects $\mathbf{c}_n^{ACS}$ (transient, reproducible, depends on current and time)

a. *Coupling currents*: Eddy currents are induced in loops among the transposed superconducting filaments in the strands, or among the strands in the cables. These currents *couple* the filaments and strands electromagnetically. They have time constants in the range of a few milliseconds (among filaments in the strands) to a few hundreds of milliseconds (among strands in cables). This contribution is only present during changes in the operating field, e.g. during energy ramp. For the typical ramp times to be used in the LHC operation they can be assumed to be fully developed in the resistive regime, that is, all inductive and shielding effects have already decayed. We also neglect the field dependence of the total resistance of the coupling current loops. With this assumption, the contribution of coupling currents to the field errors is linear with the ramp rate:

$$\mathbf{c}_n^{coupling} = \theta_m \frac{I_{inj}}{10I}\frac{dI}{dt} \tag{10}$$

where the normalization factor is used to refer the contribution to the nominal ramp rate of the LHC (10 A/s). This effect is very small and close to the measurement accuracy of the rotating coils used in the cold tests.

3) AC Long Term Effects $\mathbf{c}_n^{ACL}$ (transient, non reproducible, depends on current, time and powering history)

a. *Decay:* this component is important at injection and in all current plateaus at low field. As shown by [4] the variation of harmonics at constant current is driven by field changes on the strands caused by current redistribution in the superconducting cables. The amplitude of the current distribution process can be modeled by an equation, whose most general solution is a series of harmonics in space modulated by an exponential dependence in time. The decay phenomenon is quite complex: the current redistribution causes a change of the local field in the coil by few mT, which in turn changes the persistent currents distribution and the dc magnetization of the filaments by adding an arbitrary component to the initial magnetization state. This results in a net decrease of the average dc magnetization of the cables and an overall decrease of its contribution to the total field. Neglecting all non-linearities, we make here the simplifying assumption that the dynamics of the field follows that of a current diffusion process. The evolution follows the function [5]:

$$\mathbf{c}_n^{decay} = \delta_n\left[a_n^{\Delta}\left(1-\mathrm{e}^{-\frac{t-t_{inj}}{\tau_n}}\right)+\left(1-a_n^{\Delta}\right)\left(1-\mathrm{e}^{-\frac{t-t_{inj}}{9\tau_n}}\right)\right] \tag{11}$$

where t is the time, t_{inj} is the time at injection, τ_n is the time constant. a_n^{Δ} gives the normalized weight of the fast component of the decay and its complement to one, and $1-a_n^{\Delta}$ gives the normalized weight of the slow component. The amount of decay δ_n depends mostly on the powering history, which in practice, can be condensed to a single powering cycle characterized by the current reached at flat-top, the flat-top duration, and the pre-injection time [5].

b. *Snapback:* rapid re-establishment of the magnetization after its decay during a constant current plateau. This contribution is important at the beginning of the

acceleration ramp. Fast sextupole measurements in the LHC and Tevatron main bending dipole magnets have shown that the sextupole snap-back can be described well (within a standard deviation of 0.02 units) by an exponential fit [5]. Based on this observation, the harmonics snap-back can be modeled by:

$$\mathbf{c}_n^{snap-back} = \Delta\mathbf{c}_n^{decay} e^{-\frac{I(t)-I_{inj}}{\Delta I_n}} \quad (12)$$

where $I(t)$ is the instantaneous value of the current, I_{inj} is the injection current and $\Delta\mathbf{c}_n^{decay}$ and ΔI_n are the fitting parameters.

As a general rule, superconducting magnets (and especially dipoles and quadrupoles) are designed to achieve relative field errors of 0.1 % or better. For this reason, we can safely assume that all deviations from linearity are small perturbations of the ideal field, and that they can be added linearly to obtain the total field in the magnet. Hence, under this assumption, the field model can be given by the sum of the contributions:

$$\mathbf{c}_n = \mathbf{c}_n^{DC} + \mathbf{c}_n^{ACS} + \mathbf{c}_n^{ACL} \quad (13)$$

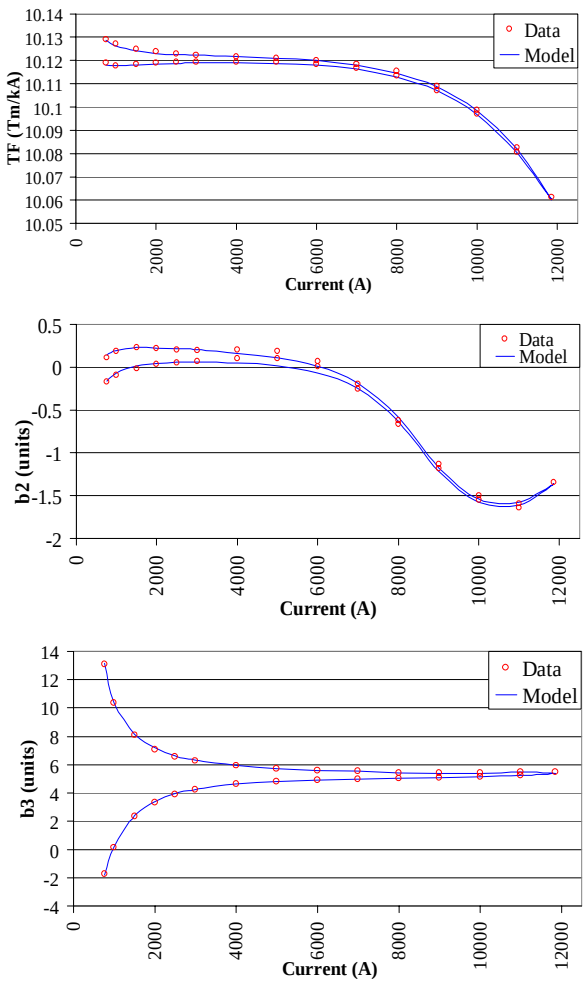

Figure 1: Modeling of the transfer function (above), the normal dipole (center) and the normal sextupole (below) for a loadline cycle.

HARMONICS FORECAST

We have performed an exercise to predict the field errors of the LHC dipoles in sector 7-8 during a ramp. In this case, only the static error components were considered i.e. the dc magnetization from persistent currents, the residual magnetization, the geometric, the iron saturation and the displacement contribution. The data consists of the integral of all the cold-tested magnets of the sector (130 apertures). The results reported in Figure 1 and 2 show that the modeling can be quite effective. The maximum error is less than 0.1 units @17mm for the harmonics in the range between injection (760A) and collision current (11850A).

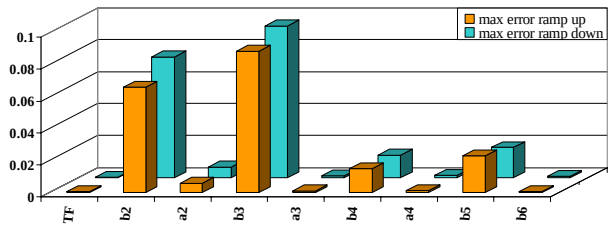

Figure 2: Maximum error between data and model in units @17mm

CONCLUSION

We have described in some detail the elements of the non-linear machinery that can provide a forecast of current ramps and corrections for the LHC control. However, the coefficients of the model are not frozen, and can be adapted. The recalibration will be based on the results of beam measurements or special measurement campaigns performed on spare and left-over magnets, using the cryogenic benches of the superconducting magnet test plant. This will allow us to refine the prediction capability, typically on a time basis of a few months.

REFERENCES

[1] S. Amet, L. Bottura, L. Deniau, L. Walckiers, 'The Multipoles Factory: An Element of the LHC Control', Proceedings to the International Conference on Magnet Technology (MT17), pp 1417-1421, Geneva Switzerland, 2001.

[2] K.H. Mess, P. Schmüser, S. Wolff, "Superconducting Accelerator Magnets", Ed. World Scientific, Singapore, 1996

[3] L. Bottura, "A Practical Fit for the Critical Surface of NbTi", Proceedings to the International Conference on Magnet Technology (MT16), pp 1054-1057, Ponte Vedra Beach USA, 1999

[4] L. Bottura, M. Breschi, M. Fabbri, "Analytical Calculation of Current Distribution in Multistrand Superconducting Cables", Proceedings to the Applied Superconductivity Conference (ASC), pp 1710-1713, Houston Texas USA, Aug 2004

[5] L. Bottura, T. Pieloni, N. Sammut, 'Scaling Laws for the Field Quality at Injection in the LHC Dipoles', CERN Project Note 361, 2005-02-21